

Dynamical coding of sensory information with competitive networks

M.I. Rabinovich^{a*}, R. Huerta^{a,b}, A. Volkovskii^a, H.D.I. Abarbanel^{a,c}, M. Stopfer^d,
G. Laurent^d

^a*Inst. for Nonlinear Science, University of California, San Diego, La Jolla, CA 92093, USA*

^b*GNB, E.T.S. de Ingeniería Informática, Universidad Autónoma de Madrid, 28049 Madrid, Spain*

^c*Department of Physics and Marine Physical Laboratory, Scripps Institution of Oceanography, University of California, San Diego, La Jolla, CA 92093, USA*

^d*Division of Biology, California Institute of Technology, Pasadena, CA 91125, USA*

Received 27 August 2000; accepted 12 October 2000

Abstract – Based on experiments with the locust olfactory system, we demonstrate that model sensory neural networks with lateral inhibition can generate stimulus specific identity-temporal patterns in the form of stimulus-dependent switching among small and dynamically changing neural ensembles (each ensemble being a group of synchronized projection neurons). Networks produce this switching mode of dynamical activity when lateral inhibitory connections are strongly non-symmetric. Such coding uses ‘winner-less competitive’ (WLC) dynamics. In contrast to the well known winner-take-all competitive (WTA) networks and Hopfield nets, winner-less competition represents sensory information dynamically. Such dynamics are reproducible, robust against intrinsic noise and sensitive to changes in the sensory input. We demonstrate the validity of sensory coding with WLC networks using two different formulations of the dynamics, namely the average and spiking dynamics of projection neurons (PN). © 2000 Elsevier Science Ltd. Published by Éditions scientifiques et médicales Elsevier SAS

competitive dynamics / sensors / coding / olfaction

1. Introduction

As multi-electrode recordings show, the representation of odors in the antennal lobe (AL) of insects comes through both identity and temporal encoding: each odor is characterized by a specific highly reproducible sequence of firing of specific projection neurons (PNs) [7, 8, 13]. Such identity-temporal encoding has many advantages discussed below. To build a corresponding dynamical theory of such an encoding, we must first understand the main principles on which the dynamics of the sensory neural networks is based. Taking into account the results of neurophysiological experiments, we can formulate at least three conditions that a model of early olfactory networks should satisfy: (i) reproducibility of sensory representations from one experiment to another; (ii) robustness of representations against internal and external fluctuations; (iii) sensitivity to changes in the stimuli, including the ability to detect small differences between different stimuli.

Several modes of activity in neural networks are traditionally proposed as principles for representing sensory information. However, the existing encoding schemes do not completely satisfy direct experimental observations or conditions (i)–(iii) formulated above. We show here that a model sensory network with lateral inhibition may use a specific dynamical mode of activity (winner less competition, WLC) to represent stimuli. Stimulus-dependent WLC dynamics can represent olfactory information in a way very similar to that expressed by AL circuits.

In autonomous nonlinear systems, the dynamics which we call ‘winner-less competition’ has been observed in experiments with rotating thermal convection [2], and in different model systems, such as the Gause-Lotka-Volterra model of competition between three species [9], and the cyclic model of central pattern generators [6]. In a very general form the competitive dynamics can be described by the equation:

$$\frac{dx_i}{dt} = x_i \left[1 - \sum_{j=1}^N \rho_{ij} x_j \right] \quad (1)$$

where: x_i , $i = 1, \dots, N$ are the dynamical variables (e.g. the population of species in the Gause-Lotka-Volterra model of competition), $\rho_{ij} \geq 0$ are the

* Correspondence and reprints.

E-mail address: rabin@landau.ucsd.edu (M.I. Rabinovich).

coefficients of interaction between the populations, and N is the number of competing species.

The behavior of this system depends on the values of parameters ρ_{ij} . As shown for $N=3$ [9], the system may have an equilibrium point with all three species present ('weak competition'), three single-species stable equilibrium points to one of which the system converges depending on the initial conditions (multistability or Hopfield-like systems [5] with symmetric connections $\rho_{ij} = \rho_{ji}$), and a parameter region where no stable equilibrium point exists and the cyclic solution implies oscillations in the population of species ('winner-less competition'). The last case corresponds to asymmetric connections or asymmetric synapses [11].

The representation of winner-less competition in the phase space of an autonomous dynamical system is a closed orbit in the vicinity of a heteroclinic loop (for details see, for example [4]). In our example (Equation (1) with $N=3$), the heteroclinic loop is an orbit consisting of three saddle equilibrium points and separatrices connecting them (see figure 1a).

For sensory neural networks, heteroclinic loops can consist of saddle limit cycles (instead of steady states) connected by separatrices (see figure 1b). The limit cycles in this case correspond to spiking activity in quasi-steady states.

It is important to note that if the heteroclinic loop or the closed trajectory in its neighborhood is a global attractor in the phase space of the sensory network, any transient behavior converges to this attractor when time increases. Another important feature of the winner-less competition behavior is the structural stability of the corresponding attractor: the global attractor exists in a wide region of parameter space.

From a nonlinear dynamics point of view, the central result is the following. In the phase space of a non-autonomous WLC system (i.e. when a stimulus is present), a new global attractor replaces the heteroclinic trajectory seen in the autonomous case (i.e. no stimulus); the structure of this new attractor determines the sequence of firing, which uniquely depends on the stimulus. Thus, each stimulus may be specifically represented as the time sequence of active and inactive states of different units in the network. This sequence can thus be used for representation and recognition of sensory information.

Note, finally, that such WLC behavior is expressed if the neural network has non-symmetric inhibitory connections between units, and the connections can form a closed circuit. We now study

the WLC dynamics of AL networks using both average and spiking activity of the units in our model.

2. Materials and methods

2.1. WLC with averaged dynamics

We begin by considering one triplet of coupled neurons and characterize each projection neuron by its 'activity' $Y_i(t) \geq 0$. The interaction among neurons is quadratic in $Y_i(t)$, reflecting the simplified inhibitory synaptic connections. These $Y_i(t)$ are taken to satisfy dynamical equations of the form:

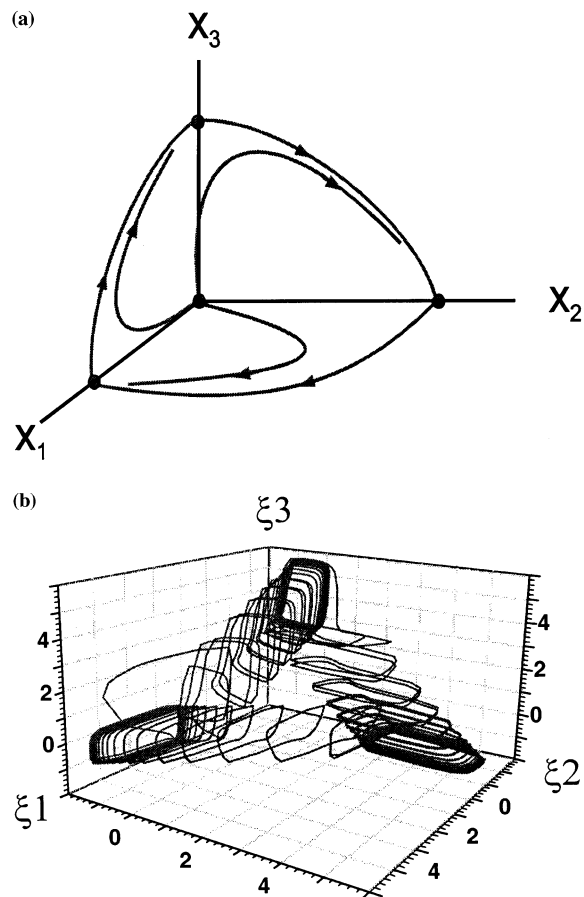


Figure 1. The phase portrait corresponding to the autonomous WLC dynamics of Equation (1): a three-dimensional case (a), and the projection of a nine-dimensional heteroclinic orbit of three inhibitory coupled FitzHugh-Nagumo spiking neurons with inhibitory connections in a three dimensional space (b). The variables ξ_1 , ξ_2 , ξ_3 are linear combinations of the actual phase variables of the system.

$$\frac{dY_i(t)}{dt} = Y_i(t) \left\{ \sigma(E_i(t) + S_i(t)) - \sum_{k=1}^3 \rho_{ik} Y_k(t) \right\}, \quad (2)$$

where $\sigma(x)$ is the threshold function:

$$\sigma(x) = 1 - \frac{2}{1 + \exp(10(x - 0.4))},$$

and

$$E_i(t) = g_e \sum_{k \neq i} Y_k(t),$$

g_e is the strength of the excitatory connection, $S_i(t)$ is the input sensory stimulus arriving at neuron i through an excitatory synapse, $E_i(t)$ is the excitatory input from other projection neurons in the ensemble, and the ρ_{ik} are the strengths of the inhibitory synapses.

When there is no stimulus, $S_i = 0$, the threshold function $\sigma(x) \approx -1$, each activity is strongly damped, and all $Y_i(t) \rightarrow 0$. When the input activates neuron i , $\sigma(x) \approx +1$, the dynamics of that

neuron near $(0,0,0)$ – the rest state – becomes unstable and its activity grows exponentially fast towards one of the unstable equilibrium states $(1,0,0)$, $(0,1,0)$, or $(0,0,1)$. Because these equilibrium states are unstable, the trajectory approaches one of them, for example $(0,1,0)$, but never reaches it before the instability of that state drives it towards another, for example, $(0,0,1)$. The activity $Y_3(t) \approx 1$ enters the equations for both $Y_1(t)$ and $Y_2(t)$ and destabilizes the other equilibrium points. The trajectory, determined in detail by the stimulus pattern (S_1, S_2, S_3) , continues to traverse the heteroclinic region until the stimulus is removed at which time the system returns to the resting state.

An input pattern (for example, a spike train from afferents integrated to provide a pulse of some longer duration) produces a well determined, reproducible pattern of firing both in space (neuron identity) and time. Different input patterns will give rise to different sequences of waveforms

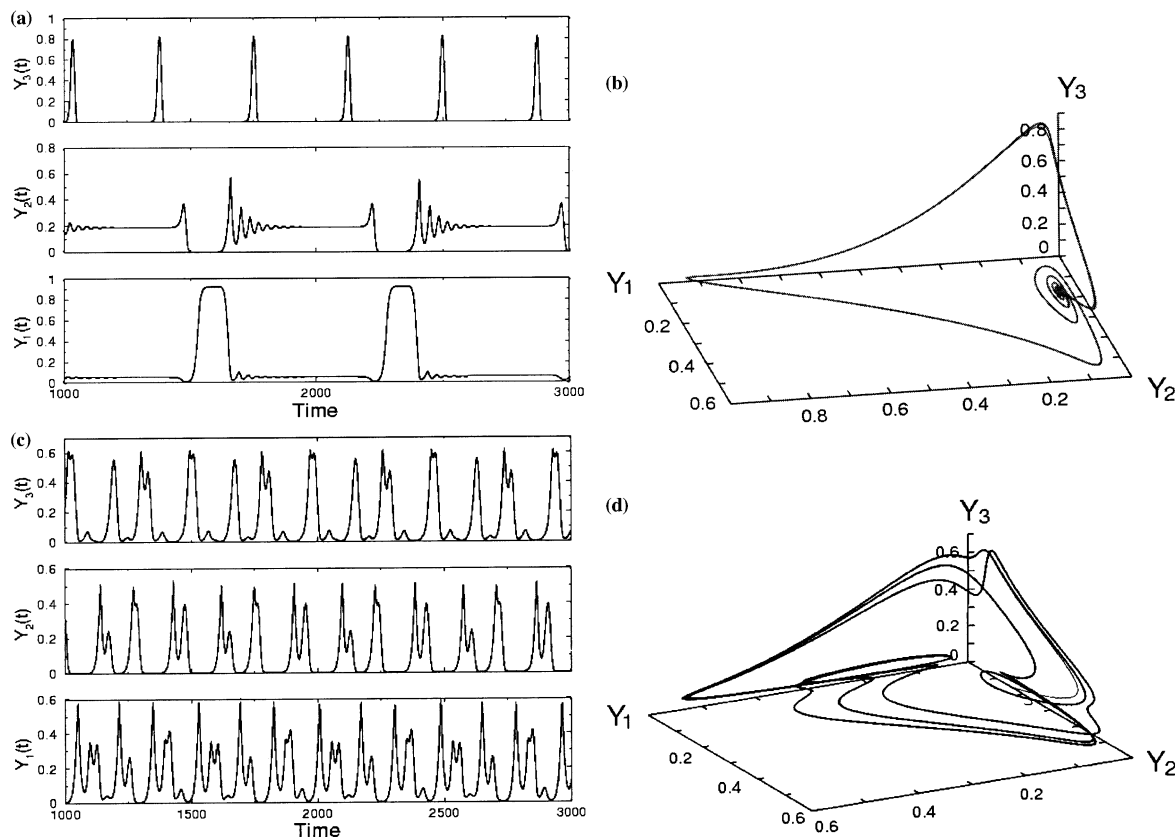


Figure 2. (a) Time series of a single triplet of averaged neurons, Equation (2), with inputs $S_i = (0.72, 0.089, 0.737)$. (b) The state space orbit $(Y_1(t), Y_2(t), Y_3(t))$ for the time series shown in a. (c) Time series of a single triplet of averaged neurons, Equation (2), with inputs $S_i = (0.189, 0.037, 0.342)$ (another ‘odor’). (d) The state space orbit $(Y_1(t), Y_2(t), Y_3(t))$ for the time series shown in c. We chose $\rho_{11} = \rho_{22} = \rho_{33} = 1$, $\rho_{12} = \rho_{23} = \rho_{31} = 5$, and $\rho_{21} = \rho_{32} = \rho_{13} = 0.2$ along with $g_e = 4$.

in each individual neuron. In *figure 2*, we show the sequence of waveforms arising from the input choice $S_i = (0.72, 0.089, 0.737)$ over a fixed time interval (zero otherwise). Its phase space portrait $(Y_1(t), Y_2(t), Y_3(t))$ is displayed in *figure 2b*. One can see the elements of sequential firing observed experimentally as well as the trajectory transformation along the ‘ribs’ of the heteroclinic connections between the unstable equilibrium points of our system. If we change the stimulus to $S_i = (0.189, 0.037, 0.342)$ representing a different ‘odor’, the pattern changes markedly (see *figure 2c, d*), as also observed experimentally [7, 13].

2.2. Sensory network with spiking dynamics

Spiking neurons or groups of synchronized spiking neurons in a network with non-symmetrical lateral inhibition may switch between active and inactive states according to the WLC dynamics. They would thus be able to encode sensory information as discussed above. The mathematical image of such switching activity is also a heteroclinic loop, but in this case the separatrices do not connect saddle equilibrium points like in *figure 1a*, but saddle limit cycles like in *figure 1b*. We simulate the WLC dynamics in a network of nine spiking FitzHugh-Nagumo neurons (see, for example [3]) with inhibitory connections as shown in *figure 3*.

The network can be described by the following equations:

$$\begin{aligned} \frac{dx_i}{dt} &= \frac{1}{\tau_1} (f(x_i) - y_i - z_i(x_i - v_{\min}) + 0.35 + S_i) \\ \frac{dy_i}{dt} &= (x_i - by_i + a) \\ \frac{dz_i}{dt} &= \frac{1}{\tau_2} \left(\sum_j g_{ji} G(x_j) - z_i \right) \end{aligned} \quad (3)$$

where x_i denotes the membrane potential, y_i is the recovery variable, and z_i represents the synaptic currents in the i -th neuron, modeled by first order kinetics. $f(x) = x - \frac{1}{3}x^3$ is the internal nonlinearity of the FitzHugh-Nagumo model. In this case, for the sake of simplicity, we introduce the stimulus as a constant current. We use a step function in the form:

$$G(x) = \begin{cases} 0, & x \leq 0 \\ 1, & x > 0 \end{cases}$$

to simulate the synaptic connection. $S_i \geq 0$ is the external excitation (stimulus) and g_{ji} is the strength

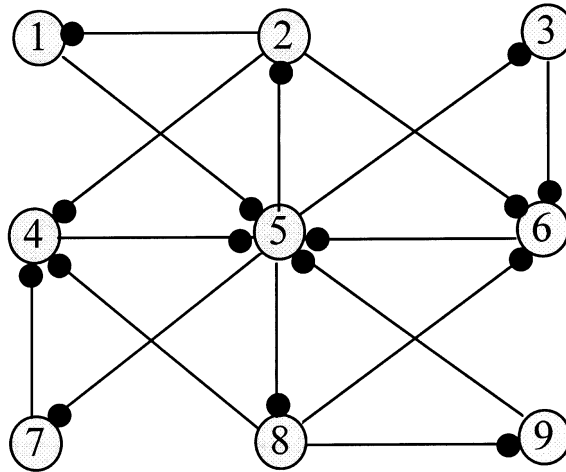


Figure 3. A network of nine FitzHugh-Nagumo neurons with inhibitory connections, in which all connections are arranged into closed loops. In this case all elements of the network can be involved in cooperative WLC dynamics.

of synaptic inhibition: $g_{ji} = 2$ if j -th neuron inhibits i -th, otherwise g_{ji} vanishes. The other parameters are set as follows: $a = 0.7$, $b = 0.8$, $\tau_1 = 0.08$, $\tau_2 = 3.1$, $v_{\min} = -1.5$.

Numerical simulations show that the network can produce different spatio-temporal patterns in response to different stimuli. *Figure 4* presents examples of spatio-temporal activity patterns corresponding to two different stimuli. The system was in the resting state ($x_i \cong -1.2$, $y_i \cong -0.62$, $z_i = 0$) before the stimulus came on at $t = 0$. As one can see, the stimulus-evoked patterns are considerably different and, therefore, distinguishable. Experimental recordings made in locusts’s AL neurons (*figure 5*) are consistent with such dynamics (see also [7, 12, 13]).

3. Results

In order to characterize the neural network as a signal-processing device, it is necessary to define first what kind of information representation is used at the input and at the output; in other words we must define the input and output coding spaces. In our model (Equation 3) each element may receive an excitatory input signal S_i (see *figure 6*). Suppose that the input signal is binary (each element is either excited or not). In this case we can represent the input to the whole network as a nine digit binary number $d = d_1, \dots, d_9$: $d_i = 1$, if $S_i > 0$ and $d_i = 0$, if $S_i = 0$, for $i = 0, \dots, 9$. The total number of different inputs is $2^9 = 512$. The output

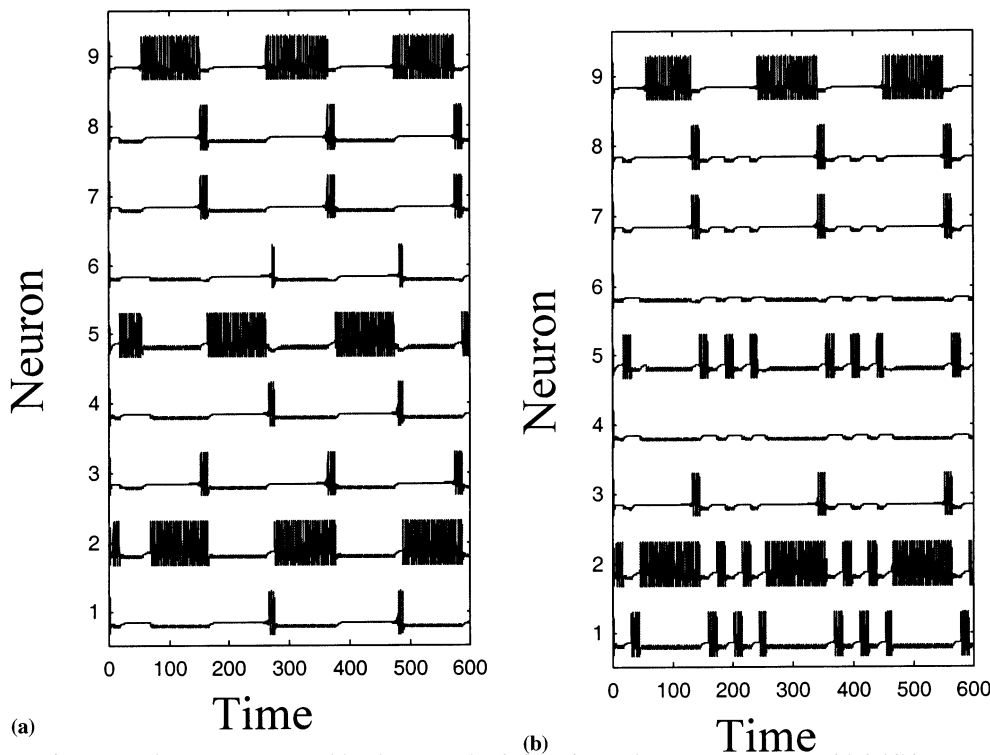


Figure 4. The spatio-temporal patterns generated by the network of nine FitzHugh-Nagumo neurons with inhibitory connections and the external stimulus: $S_1 = 0, S_2 = 0.15, S_3 = 0, S_4 = 0, S_5 = 0.15, S_6 = 0, S_7 = 0, S_8 = 0, S_9 = 0$ (a), and $S_1 = 0.15, S_2 = 0.15, S_3 = 0, S_4 = 0, S_5 = 0.15, S_6 = 0, S_7 = 0, S_8 = 0, S_9 = 0$ if $S_j = 0$ (b).

of each element (x_i) is also considered to be binary (each element is either active or not). At any given time, the outputs of all nine elements of the network can be given as a nine digit binary number $b = b_1, \dots, b_9$ with $b_i = 1$, if $b_i > 0$ and $b_i = 0$, if $x_i \leq 0$. Due to the system's dynamics the output signals change over time. This process can be represented as a sequence of binary numbers $Q_k^L = b^1; b^2; \dots; b^L$, where L is the length of the sequence and k is the output sequence index.

To demonstrate the robustness and reproducibility of the representation of the stimulus by the network we generated randomly ten input signals $d^1 \dots d^{10}$ and ran the simulation with model (Equation 3) M times for each input d^i with different initial conditions randomly set inside a sphere with radius r and centered at zero. In each simulation the output sequence Q_k^L was recorded. After all output sequences corresponding to inputs $d^1 \dots d^{10}$ and all initial conditions were generated, a total of N different output sequences $Q_k^L, k = 1, \dots, N$ were detected. The calculations were performed with two different radii r to test the reliability of the representation against noise.

To illustrate the dependence of the information content on the length of the output sequence, we calculate the average mutual information I :

$$I = \sum_{i=1}^{10} \sum_{j=1}^N P(d^i, Q_j^L) \log \frac{P(d^i, Q_j^L)}{P(d^i)P(Q_j^L)}$$

where $P(d^i, Q_j^L)$ is the joint probability distribution $P(d^i)$ is the probability of input signal d^i (we consider d^i to be uniformly distributed, so $P(d^i) = 1/D, D$ is the number of different inputs), $P(Q_j^L)$ is the probability of output sequence Q_j^L .

The average mutual information as a function of the output sequence length L for different radii r of initial conditions is presented in figure 7. One can see that the average mutual information reaches its maximum value (equal to the entropy of the input signal), if the length of the output sequences L is sufficiently long (in this case $L \geq 4$).

These simulations have the following two implications: Firstly, in order to maximize the average mutual information between these ten specific given inputs and the output sequences, an output sequence larger than three is required; and, secondly, regardless of the noise radius, the information saturates for output sequences greater than

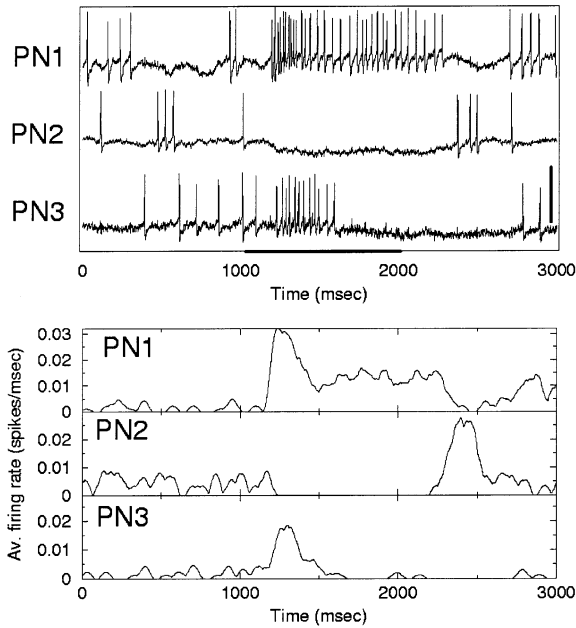


Figure 5. Simultaneous intracellular recordings from three PN neurons in the Antennal Lobe of the locust (top panel) in the presence of an external olfactory input between 1000 and 2000 ms and smoothed peri-stimulus time histograms (lower panel). Vertical calibration (top): 30 mV.

three. The bottom line is that temporal encoding is required in this type of systems to achieve a good representation of the input data.

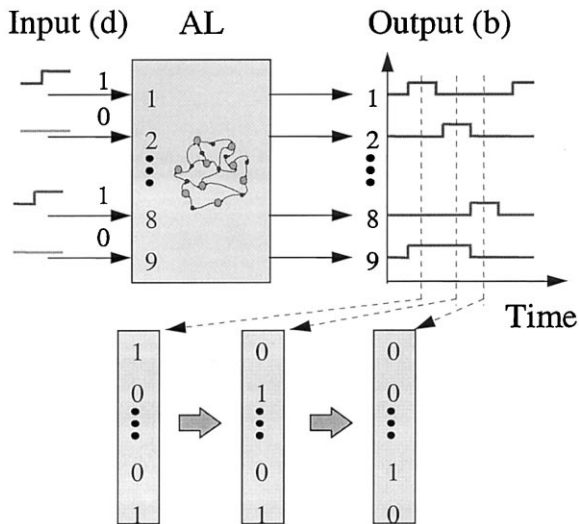


Figure 6. The transformation of an ‘identity’ code into an ‘identity-temporal’ code in the AL.

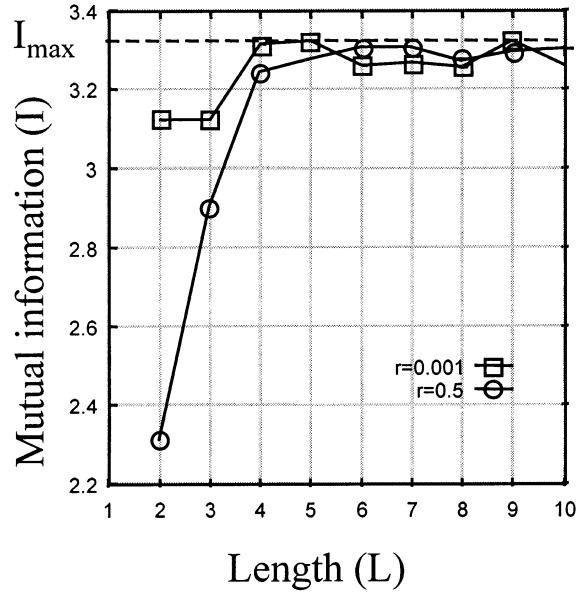


Figure 7. Average mutual information as a function of output sequence length L .

4. Discussion

We have proposed a new class of neural network models whose stimulus-dependent dynamics reproduce the rich spatio-temporal features observed in insect olfactory systems. The principle of such a representation (which we call stimulus-dependent winner-less competition) relies on the fact that specific trajectories act as global attractors in state space. This global behavior corresponds to experimental data, showing that activity proceeds across parts of the AL by the sequential activation and deactivation of sub-groups of neurons. This ‘activation path’ within the network (or correspondingly the global attractor which appears under the action of the stimulus in the neighborhood of the heteroclinic orbit) is determined by and thus ‘represents’ the stimulus. Because this attractor is global, such representation is robust against fluctuations and noise (see [10]). A stimulus can thus be thought of as an informational signal that reorganizes the global attractor in a stimulus-specific manner, forcing the system to evolve through state space along a complex, but deterministic path joining unstable ‘saddle states’. Once the stimulus ceases, each active neuron returns to its baseline activity, controlled by intrinsic properties, basal connection strengths and noise.

The properties of these simplified models can also emerge from more realistic networks domi-

nated by asymmetrical inhibitory connections. In particular, if the system is large, it is not necessary that the network topology is closed. A large network with sparse, random connections will exhibit the same stimulus dependent sequential activation and deactivation of sub-groups of neurons. Finally our central idea does not depend on the nature of the stimulus; it may thus apply to non-olfactory brain circuits as well, and explain experimental observations of flipping between quasi-stationary states of activity in monkey cortex [1].

Acknowledgements

This work was supported in part by the US Department of Energy, Office of Basic Energy Sciences, Division of Engineering and Geosciences, under grant DE-FG03-90ER14138, and by NIDCD (Laurent).

References

- [1] Abeles M., Bergman H., Gat I., Meilgison I., Seidemann E., Tishby N., Vaadia E., Cortical activity flips among quasi-stationary states, *Proc. Nat. Acad. Sci. USA* 92 (1995) 8616–8620.
- [2] Busse F.H., Heikes F.H., Convection in a rotating layer: a simple case of turbulence, *Science* 208 (1980) 183–187.
- [3] Cronin J., *Mathematical Aspects of Hodgkin-Huxley Neural Theory*, Cambridge University Press, Cambridge, 1987.
- [4] Grossberg S., Decision, patterns and oscillations in nonlinear competitive systems with applications to Volterra-Lotka systems, *J. Theor. Biol.* 73 (1978) 101–130.
- [5] Hopfield J.J., Neural networks and physical systems with emergent computational abilities, *Proc. Nat. Acad. Sci. USA* 79 (1982) 2554–2558.
- [6] Kleinfeld D., Sequential state generation by model neural networks, *Proc. Nat. Acad. Sci.* 83 (1986) 9469–9473.
- [7] Laurent G., Wehr M., Davidovitz H., Temporal representations of odors in an olfactory network, *J. Neurosci.* 16 (1996) 3837–3847.
- [8] Laurent G., A systems perspective on early olfactory coding, *Science* 286 (1999) 723–728.
- [9] May R.M., Leonard W.I., Nonlinear aspects of competition between three species, *SIAM J. Appl. Math.* 29 (1975) 243–253.
- [10] Rabinovich M.I., Huerta R., Volkovskii A.R., Abarbanel H.D.I., Laurent G., Sensory Coding with Dynamically Competitive Networks, *Electronic Preprints*, 1999, <http://arXiv.org/abs/neuro-sys/9905002>.
- [11] Sompolinsky H., Kanter I., Temporal association in asymmetric neural networks, *Phys. Rev. Lett.* 57 (1986) 2861–2864.
- [12] Stopfer M., Laurent G., Short-term memory in olfactory network dynamics, *Nature* 402 (1999) 664–668.
- [13] Wehr M., Laurent G., Odor encoding by temporal sequences of firing in oscillating neural assemblies, *Nature* 384 (1996) 162–166.